LA-UR- 97-2643

Approved for public release; distribution is unlimited.

Title: SOURCE AND PATH EFFECTS ON REGIONAL PHASES IN CHINA.

CONF-970967--

Author(s): WILLIAM S. PHILLIPS, GEOPHYSICS GROUP EES-3, MS C335, LOS ALAMOS NATIONAL LAB

GEORGE E. RANDALL, GEOPHYSICS GROUP EES-3, MS C335, LOS ALAMOS NATIONAL LAB

HANS E. HARTSE, GEOPHYSICS GROUP EES-3, MS C335, LOS ALAMOS NATIONAL LAB

STEVEN R. TAYLOR, GEOPHYSICS GROUP EES-3, MS C335, LOS ALAMOS NATIONAL LAB

HOWARD J. PATTON, GEOPHYSICS GROUP EES-3, MS C335, LOS ALAMOS NATIONAL LAB

Submitted to: PROCEEDINGS OF THE 19TH SEISMIC RESEARCH SYMPOSIUM ON MONITORING A COMPREHENSIVE TEST BAN TREATY.

Los Alamos
NATIONAL LABORATORY

Form 836 (10/96)

DISCLAIMER

SOURCE AND PATH EFFECTS ON REGIONAL PHASES IN CHINA

W.S. Phillips, G.E. Randall, H.E. Hartse, S.R. Taylor and H.J. Patton
Geophysics Group EES-3, Los Alamos National Laboratory

Sponsored by the U.S. Department of Energy, Contract W-7405-ENG-36
CTBT Research and Development Program, ST482A

ABSTRACT

As part of the CTBT Research and Development regional characterization effort, we are assembling, organizing and analyzing geological, geophysical, and seismic data for inclusion in a knowledge base for China. Guided by the USGS Preliminary Determination of Epicenters (PDE) and Chinese State Seismological Bureau event catalogs, we have collected seismic data from 11 Chinese Digital Seismic Network (CDSN) stations as well as IRIS stations AAK, TLY, ULN and NIL from adjoining regions. Using the published event locations and origin times, we identify *Pn*, *Pg*, *Sn*, and *Lg* phases, construct travel time curves, and estimate apparent velocities from broadband and short-period seismograms. Following this, we collect amplitudes of regional seismic phases and associated noise levels using bandpassed waveforms. Studies of path-specific propagation of the seismic phases have mapped blockages and have generated corrections useful in reducing scatter in magnitude estimates and in discriminant ratios. Such path corrections reduce RMS distance- and m_b-corrected Lg amplitude to as much as 60% of its original level ($\log_{10}$ domain). Path corrections are less effective with *Pn* data. We also study source scaling effects on these data which will allow us to refine path corrections further.

Key Words: regional seismic characterization, China, path effects, source scaling

OBJECTIVE

We continue to characterize the regional excitation and propagation of seismic waves in China with sufficient accuracy to explain observed seismic data, and to detect, locate, and discriminate seismic events for the verification of a Comprehensive Test Ban Treaty (CTBT). Our primary source of seismic data has been the stations of the Chinese Digital Seismic Network (CDSN), augmented by nearby IRIS stations. Using seismic waveforms and event locations from the USGS PDE and Chinese seismicity catalogs, we have identified *Pn*, *Pg*, *Sn*, *Lg*, Love and Rayleigh phases and picked arrival times and amplitudes for the body waves. Analysis of these arrival times will provide travel time and travel time corrections for large, well-located events to improve regional location. Amplitudes are analyzed to calibrate magnitude scales and for use in discrimination research.

RESEARCH ACCOMPLISHED

Past Regionalization Efforts. Randall et al. (1995) and Randall et al. (1996) have reported on initial data gathering and analysis efforts, including digital geology and cultural data (through USGS, Flagstaff), compilation of mine locations and practices, seismic event cluster analysis to further identify mining regions, magnitude scale calibration and detection threshold studies. Details can also be found in Hartse et al. (1996), Hartse et al. (1997abc) and Taylor and Hartse (1996, 1997).

Data Collection and Processing. We have collected and continue to process data from 11 CDSN and 4 IRIS stations in and around China (Table 1, Figure 1). We began working with data from western China (stations WMQ and AAK) and now better cover the central and eastern regions. Data contain short-period, long-period and broadband recordings. We use PDE and SSB catalogs to identify and request data for events out to 2500 km, magnitudes 3.8 and up (PDE) and 2.0 and up (SSB).

Surface Wave Dispersion. We are compiling short-path (under 1000 km) surface wave dispersion results for western China. For areas of interest, we hope to improve on the 5° resolution available from longer path studies (Ritzwoller and Levshin, 1997). Initial results from WMQ clearly show effects of the Junggar basin for periods less than 20 s. Further details may be found in this volume (Jones and Patton, 1997).

Empirical Path Correction Using Topographic Data. We have evaluated empirical path correction methods of Zhang et al. (1996) using correlations with topography as well as basin and crustal thickness to reduce the scatter of discriminant ratios in western China. Physical data have been taken from the Cornell database (Fielding et al., 1993). We find distance-weighted topography and basin thickness corrections improve the separation between earthquake and nuclear test *Pg/Lg* discriminants in 1.5-3 and 2-4 Hz bands at WMQ. We find no improvement for data recorded at AAK. Details of this study may also be found in this volume (Hartse et al. 1997b, also see Hartse et al. 1997c).

Empirical Path Corrections Based on Regional Seismic Data. Taking a different approach from Zhang et al. (1996), we have examined spatial distributions of amplitudes of regional phases to find coherent patterns that can be used as path-effect corrections. For example, a well-known path effect is the blockage of *Lg* across the edge of the Tibetan Plateau (e.g. Rapine et al. 1997). Seismograms recorded at LZH for events in eastern Tibet and the Baikal Rift illustrate this effect (Figure 2). We discuss the path-correction method and initial results further in the following.

To estimate path-correction factors for a given station, we first correct the amplitude logarithm for source size by subtracting the magnitude (m_b), followed by a correction for distance via a straight line fit in the log-log domain. As shown by Baker and Minster (1996) for discriminant ratios, patterns often emerge when such residuals are plotted on a map. These values are then smoothed spatially by averaging results for all events that fall within a 250 km circle that moves around a geographical grid (Figure 3). The smoothing is only allowed when there are more than a threshold number of crustal events (currently 5) inside the circle. Event depths are limited to under 50 km. Our assumption is that the smoothing averages out source and depth effects, leaving an estimate of the path effect that can be used for correcting magnitude estimates and discriminants.

We have applied this method to 1-2 Hz, *Lg* and *Pn* data from 6 stations in and near China (LZH, XAN, ENH, WMQ, AAK and NIL) using PDE catalog events recorded from 1986 to the present, available from the IRIS database. Spatial patterns are most apparent for the *Lg* phase. Results for LZH are plotted in Figure 4. The standard deviation of distance-corrected, log amplitude minus m_b, is reduced from 0.53 to 0.37 after applying the path correction to LZH data. Scatter reduction quantified by the ratio of standard deviations, after versus before path correction, is summarized in Table 2. We also include results for the *Pn/Lg* ratio, formed after correcting each phase independently.

Our amplitude correction patterns resemble the variation in coda Q throughout China found by Jin and Aki (1988). However, correcting LZH, 1-2 Hz, *Lg* minus m_b data using these Q values only reduced the RMS scatter to 90% of the original value. The coda Q correction worked well for paths to the southwest (E. Tibet) but poorly for paths to the northeast.

We have successfully applied the path correction technique to 3-6 Hz *Pg/Lg* discriminant ratios including Lop Nor events using data from AAK (see Hartse et al., 1997b, this volume). In contrast, empirical topographic techniques performed poorly with data from this station. The path correction technique could not be applied to Soviet test discrimination using WMQ data because no earthquakes occurred near the test site that could be used to calibrate those paths.

Source Scaling Corrections. The empirical path correction method outlined above does not account for the effect of source scaling. We evaluate this effect by inverting WMQ data for regional Q and source scaling terms as a function of frequency, assuming standard source models. We plan to combine results of the source and path studies to refine correction values. Details of the source scaling study can be found in this volume (Hartse et al., 1997b, also see Taylor and Hartse, 1997).

RECOMMENDATIONS AND FUTURE PLANS

We will continue the assembly and analysis of regional information, and refine models by comparing synthetics with real data. Waveform modeling will be employed to characterize seismic sources and attempt to constrain event depths. We will continue to identify propagation issues and details relevant to discrimination and to identify mining events using waveform correlation and clustering techniques. We will begin to collect and process data from additional regions of interest. We will also begin to use data from portable deployments and temporary arrays. Results will be organized in a form suitable for use by AFTAC in their routine processing and special event studies.

ACKNOWLEDGMENTS

We thank the staff of the IRIS Data Management Center for help with our data requests. Maps were created using Global Mapping Tool (GMT) software (Wessel and Smith, 1991). Thanks also to Laura Jones for reviewing this manuscript. This work is in support of the DOE Comprehensive Test Ban Treaty Research and Development Program, ST482A and was performed at the Los Alamos National Laboratory under the auspices of the United States DOE, Contract Number W-7405-ENG-36.

REFERENCES

Baker, G.E., and J.B. Minster, Quantifying the attenuation and blockage of Lg and robust statistical estimates of site amplifications at SCSN stations, *18th Ann. Seismic Research Symp. on Monitoring a Comprehensive Test Ban Treaty*, 1996.

Fielding, E.J., M. Barazangi and B.L. Isacks, A geological and geophysical data base for Eurasia, *Final Technical Report, ARPA NMRO F29601-91-K-DB08*, 1993.

Hartse, H.E., S.R. Taylor, W.S. Phillips and G.E. Randall, Regional seismic discrimination in central Asia with emphasis on western China, *18th Ann. Seismic Research Symp. on Monitoring a Comprehensive Test Ban Treaty*, 1996.

Hartse, H.E., S.R. Taylor, W.S. Phillips, and G.E. Randall, A preliminary study of regional seismic discrimination in central Asia with emphasis on western China, *Bull. Seism. Soc. Am.*, **87**, 551-568, 1997a.

Hartse, H.E., S.R. Taylor, W.S. Phillips and G.E. Randall, Applying source and path corrections to improve discrimination in China, *19th Ann. Seismic Research Symp. on Monitoring a Comprehensive Test Ban Treaty*, (this volume), 1997b.

Hartse, H.E., R.C. Flores and P.A. Johnson, Correcting regional seismic discriminants for path effects in western China, *Bull. Seism. Soc. Am.*, submitted June, 1997c.

Jin, A. and K. Aki, Spatial and temporal correlation between coda Q and seismicity in China, *Bull. Seism. Soc. Am.*, **78**, 741-769, 1988.

Randall, G.E., T.A. Weaver, H.E. Hartse, S.R. Taylor, R.G. Warren and A.H. Cogbill, Regional characterization of western China, *Proc. 17th Ann. Seismic Research Symp. on Monitoring a Comprehensive Test Ban Treaty*, 1995.

Randall, G.E., H.E. Hartse, W.S. Phillips and S.R. Taylor, Regional characterization of western China II, *18th Ann. Seismic Research Symp. on Monitoring a Comprehensive Test Ban Treaty*, 1996.

Rapine, R, T. Hearn, J. Wu and J. Ni, Sn and Lg propagation characteristics beneath China, *18th Ann. Seismic Research Symp. on Monitoring a Comprehensive Test Ban Treaty*, 1996.

Ritzwoller, M.H. and A.L. Levshin, Eurasian surface wave tomography: Group velocities, *J. Geophys. Res.*, submitted, March 1997.

Taylor, S.R. and H.E Hartse, Regional phase seismic detection thresholds at WMQ, *Los Alamos National Laboratory, Los Alamos, NM*, LAUR-96-395, 7pp, 1996.

Taylor, S.R. and H.E. Hartse, A procedure for estimation of source and propagation amplitude corrections for regional seismic discriminants, *J. Geophys. Res.*, submitted, June 1997.

Wessel P. and W.H.F. Smith, Free software helps map and display data, *EOS Trans AGU*, **72**, 441, 1991.

Zhang, T., T. Lay, S. Schwartz and W.R. Walter, Variation of regional seismic discriminants with surface topographic roughness in the western United States, *Bull. Seis. Soc. Am.*, **86**, 714-725, 1996.

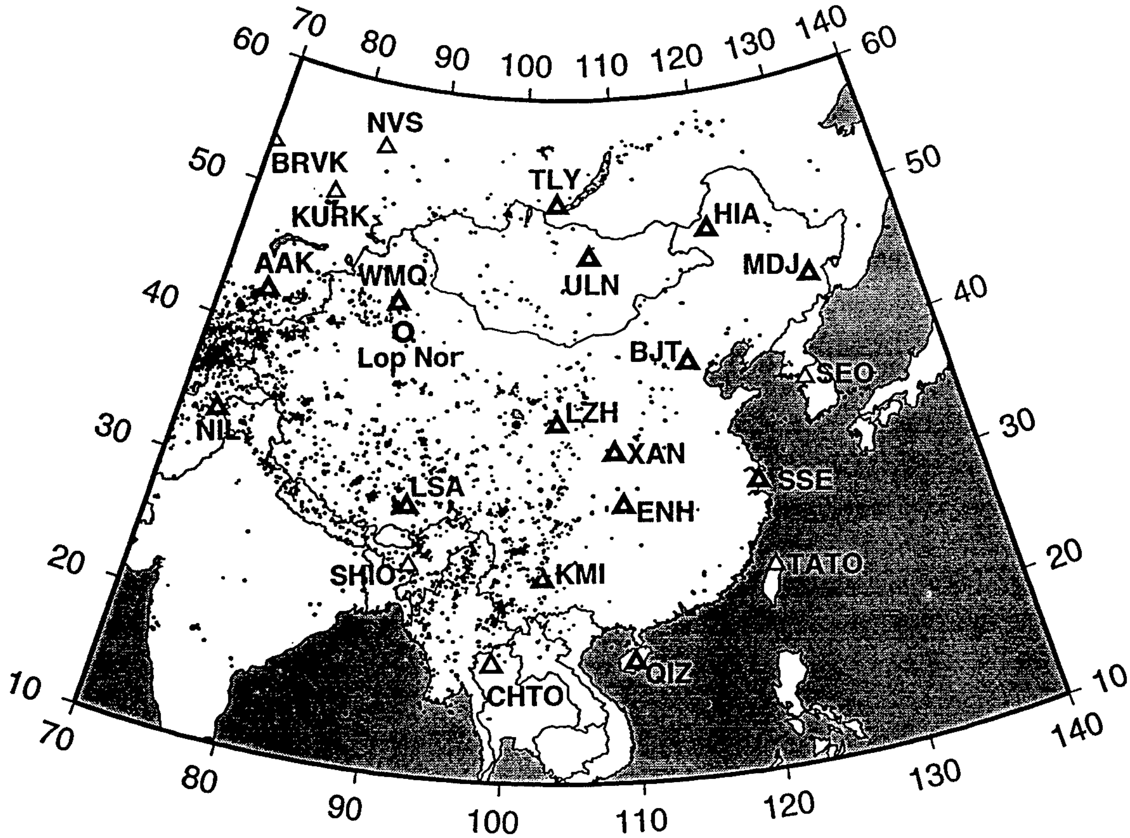

Figure 1. CDSN and IRIS stations in China and surounding areas. Bold triangles represent stations listed in Table 1, below. PDE seismicity, 1986-1996, depth less than 50 km is also included.

Table 1. Data collected to date.

Station	Location	Network	Years Collected	Total Years
AAK	Kyrgyzstan	IRIS	1990-1995	6
BJI/T	Beijing	CDSN	1986-1996	11
ENH	Enshi	CDSN	1992-1996	5
HIA	Hailar	CDSN	1988-1995	8
KMI	Kunming	CDSN	1987-1996	10
LSA	Lhasa	CDSN	1992-1996	5
LZH	Lanzhou	CDSN	1986-1996	11
MDJ	Mudanjiang	CDSN	1989-1995	7
NIL	Nilore	IRIS	1995-1996	2
QIZ	Qiongzhong	CDSN	1992-1996	5
SSE	Shanghai	CDSN	1992-1996	5
TLY	Talaya	IRIS	1990-1996	7
ULN	Ulaanbaatar	IRIS	1994-1996	3
WMQ	Urumqi	CDSN	1986-1996	11
XAN	Xi'an	CDSN	1993-1996	4

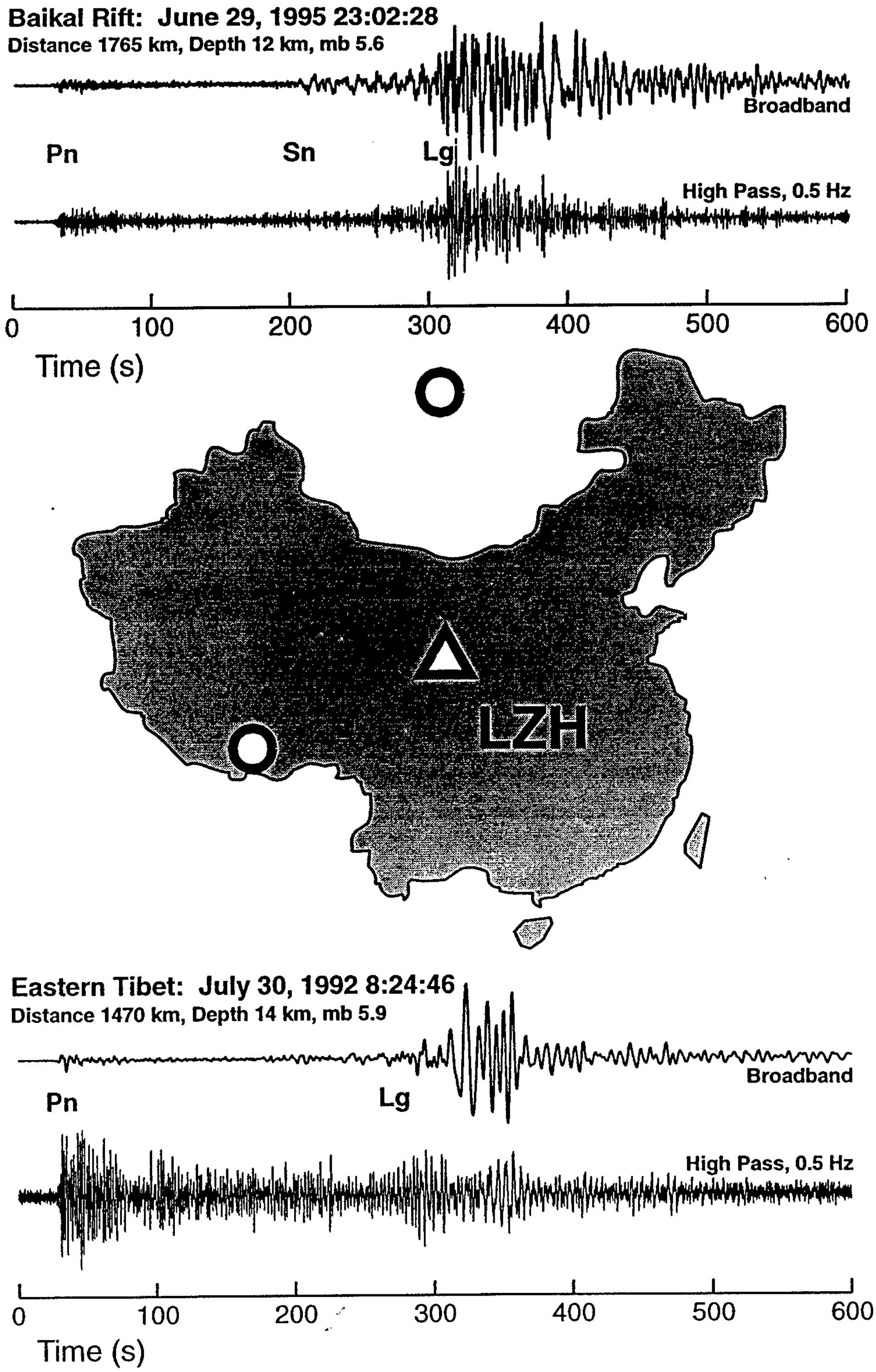

Figure 2. Broadband, vertical-component seismograms for events from the Baikal Rift (top) and eastern Tibet (bottom) recorded at LZH. In both cases, the lower trace has been high-pass filtered at 0.5 Hz. Reference times are arbitrary, but are aligned with the *Pn* arrivals.

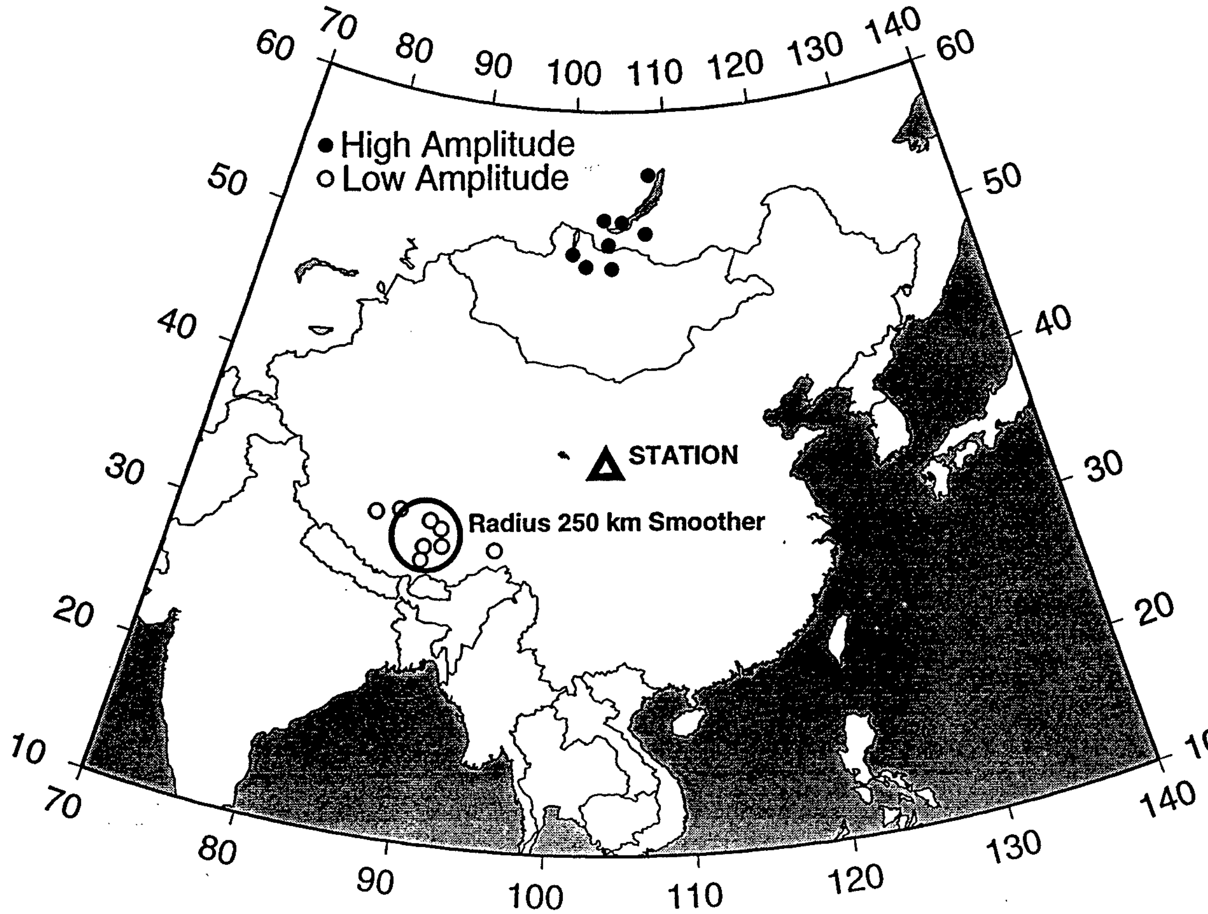

Figure 3. Illustration of the method used to create path corrections. Open and filled circles represent locations of events that generated relatively low and high amplitudes (distance-corrected log amplitude minus m_b), respectively. We require a minimum of five events within the smoothing circle to obtain a usable correction value.

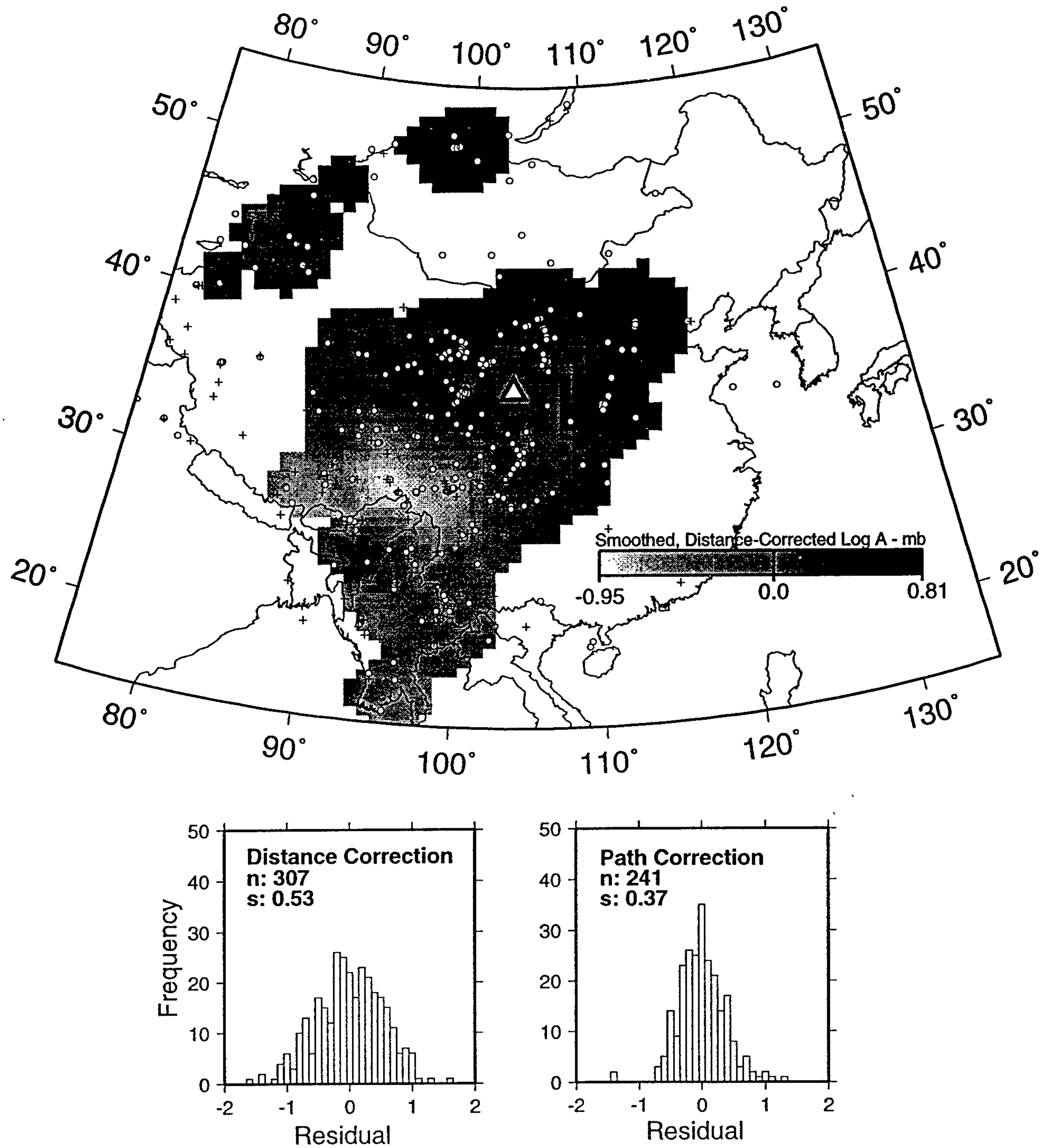

Figure 4. 1.5 Hz *Lg* path corrections (top) and log amplitude minus m_b residuals after correcting for distance (bottom left) and path (bottom right), for the station LZH, broadband vertical component. Corrections are plotted as a gray -scale image while events used in the analysis are plotted as open circles. Crosses represent events that were eliminated based on signal to noise. Histogram plots include the number of events (n) and the standard deviation of the residual (s). Similar results from other stations are summarized in Table 2.

Table 2. Ratio of standard deviations of distance-corrected, $\log_{10}$ amplitude - m_b residuals and similarly calculated *Pn/Lg* discriminant ratio residuals, after / before path correction for the 1-2 Hz band , broadband vertical component.

Station	*Lg*	*Pn*	*Pn/Lg*
LZH	0.70	0.98	0.87
XAN	0.79	0.73	0.74
ENH	0.60	0.94	0.73
WMQ	0.87	0.88	0.81
AAK	0.89	0.86	0.81
NIL	0.73	0.86	0.87

(18) DOE, XF
(19) UC-900, DOE

DOE